A physical surface-potential-based drain current model for polysilicon thin-film transistors*

Li Xiyue(李希越), Deng Wanling(邓婉玲), and Huang Junkai(黄君凯)†

Department of Electronic Engineering, Jinan University, Guangzhou 510632, China

Abstract: A physical drain current model of polysilicon thin-film transistors based on the charge-sheet model, the density of trap states and surface potential is proposed. The model uses non-iterative calculations, which are single-piece and valid in all operation regions above flat-band voltage. The distribution of the trap states, including both Gaussian deep-level states and exponential band-tail states, is also taken into account, and parameter extraction of trap state distribution is developed by the optoelectronic modulation spectroscopy measurement method. Comparisons with the available experimental data are accomplished, and good agreements are obtained.

Key words: polysilicon thin-film transistors; surface potential; drain current model; trap state distribution

DOI: 10.1088/1674-4926/33/3/034005 **PACC:** 7340N **EEACC:** 2560B

1. Introduction

In recent years, the application of poly-silicon thin-film transistors (poly-Si TFTs) has become more attractive, especially in active matrix liquid-crystal displays and organic light emitting diodes, etc. Accurate models of poly-Si TFTs are therefore needed for circuit design and simulation. Since the electrical characteristics are particularly dependent on the density of states (DOS), it is especially important to describe DOS accurately. The distribution of trap states in polysilicon film can be expressed by Gaussian deep-level states, with a peak around the midgap and exponential band-tail states near the conduction and valence band edge. This is determined by experimental methods such as capacitance–voltage relation[1], activation energy as a function of the gate voltage[2], and optical absorption[3]. These results were also confirmed by our previous experiment[4], which was accomplished using optoelectronic modulation spectroscopy (OEMS) measurements. To obtain the complete model of poly-Si TFTs, it is therefore necessary to take both the Gaussian deep-level and exponential band-tail states into account.

In poly-Si TFTs, surface potential is an important parameter. Chen *et al.*[5] and Qureshi *et al.*[6] solved the surface-potential-based model accurately. However, the exponential band-tail states were neglected and only the monoenergetic trap states were considered. Tsuji *et al.*[7] and Ikeda *et al.*[8] proposed the drain current model based on the surface potential. But in their methods, only the exponential states were taken into account and the Gaussian deep-level states were neglected. In addition, their models use iteration methods to solve the surface potential and drain current, which consumes lots of simulation time. In general, the above-mentioned methods cannot provide the complete distribution of trap states within the band gap of the polysilicon film.

In order to reduce the complexity of the calculation, it is believed that the Gaussian distribution can be regarded as a monoenergetic trap model by using the first-step approximation[9]. As a result, a complete model of DOS should include both kinds of energy trap distribution, namely the monoenergetic midgap trap and the exponential band-tail states. In this work, the surface-potential-based drain current model, including the complete distribution trap states, is proposed analytically by a single-piece formula, which is solved by the non-iteration method with efficient calculation. Furthermore, the single-piece drain current model is capable of accurately predicting experimental I–V characteristics in subthreshold, weak and strong inversion regions.

2. Theoretical bases of surface potential

With the calculation of surface potential, we assume that there is an n-type poly-Si TFT with an undoped or lightly doped body, and that the device is partially depleted. In addition, the assumption of effective medium is used here. This is suitable for small-grain TFTs which have grain sizes smaller than approximately 0.2 μm[10, 11]. The energy distribution $N_{\mathrm{b}}(E)$ of the traps can be modeled by the sum of a Gaussian distribution with a maximum at the energy E_{T} near the midgap and an exponential-like band-tail near the conduction-band edge. Herein, as in previous publications[9, 12], the Gaussian distribution is assumed as a monoenergetic midgap trap, which is considered a good approximation to the Gaussian deep-level trap states. As a result, we have

$$N_{\mathrm{b}}(E) = N_{\mathrm{T}}\delta(E - E_{\mathrm{T}}) + g_{\mathrm{c1}} \exp\frac{E - E_{\mathrm{c}}}{E_1}, \tag{1}$$

where N_{T} is the Gaussian trap density, g_{c1} is the n-type exponential states density, E_1 is the inverse slope of the states, and E_{c} is the energy in the bottom of the conduction band.

When the gate voltage is applied, the surface potential varies along the channel. Substituting Eq. (1) into the one-dimensional Poisson's equation, using the gradual channel ap-

* Project supported by the Key Project of Chinese Ministry of Education (No. 211206), the Fundamental Research Funds for the Central Universities (No. 21611422), and the Foundation for Distinguished Young Talents in Higher Education of Guangdong, China (No. LYM10032).

† Corresponding author. Email: hjkeed@163.com

Received 7 September 2011, revised manuscript received 17 November 2011

proximation and the Lambert W function, the solution of the surface potential of the poly-Si TFTs can be expressed as[13]

$$\psi_{\rm sub} = \{-W_0[f\Delta_{\rm TFT}\exp(v_{\rm G}-fA)]+v_{\rm G}-fA\}(E_1/q), \quad (2)$$

$$\psi_{\rm inv} = V_{\rm g} - V_{\rm fb} - 2\phi_{\rm t} W\sqrt{\frac{2q\varepsilon_{\rm si}n_0}{C_{\rm ox}^2\phi_{\rm t}}}\exp\frac{V_{\rm g}-V_{\rm fb}}{\phi_{\rm t}}, \quad (3)$$

where $\psi_{\rm sub}$ and $\psi_{\rm inv}$ are the surface potential in the subthreshold and strong inversion regions, respectively, W_0 is the notation of the principal-branch solution of the Lambert W function, and $V_{\rm g}$, $V_{\rm fb}$, $\phi_{\rm t}$ and $C_{\rm ox}$ is the gate voltage, flat-band voltage, thermal voltage and unit area gate oxide capacitance, respectively. Also $\Delta_{\rm TFT} = \frac{N_{\rm TA0}}{N_{\rm T}}$, $A = \frac{-\phi_{\rm t}\ln(1+K_{\rm m})}{E_1/q} - \frac{N_{\rm TA0}}{N_{\rm T}}$, $K_{\rm m} = 0.5\exp[(E_{\rm T}+E_{\rm f})/kT]$, $G = \sqrt{\frac{2q\varepsilon_{\rm si}N_{\rm T}}{C_{\rm ox}^2(E_1/q)}}$, $v_{\rm G} = (\frac{V_{\rm g}-V_{\rm fb}}{E_1/q}+\frac{G^2}{2}) - G\sqrt{\frac{V_{\rm g}-V_{\rm fb}}{E_1/q}+\frac{G^2}{4}}$, $f = G/(2\sqrt{(V_{\rm g}-V_{\rm fb})/(E_1/q)+G^2/4})$, $N_{\rm TA0} = g_{\rm c1}\frac{\pi kT}{\sin(\pi kT/E_1)}\exp\frac{E_{\rm f}-q\phi_{\rm n}-E_{\rm c}}{E_1}$, $n_0 = n_{\rm i}\exp\frac{-\phi_{\rm n}+E_{\rm f}/q}{\phi_{\rm t}}$, with $E_{\rm f}$, $\phi_{\rm n}$ and $n_{\rm i}$ the Fermi level energy, channel potential and intrinsic carrier concentration, respectively.

In the transition region of the two operation regions, both the free charge and trap states contribute to the characteristics, so the following function is used to link the different regions[13]

$$\psi_{\rm s} = \frac{1}{m}\ln\frac{1}{1/\exp(m\psi_{\rm inv})+1/\exp(m\psi_{\rm sub})}, \quad (4)$$

where m is a parameter to ensure which operation regions $\psi_{\rm s}$ should approximate to. It should be noted that Equation (4) is capable of calculating the surface potential, including both kinds of trap states, accurately and explicitly, which also serves as an important tool for the drain current model.

3. Drain current model

According to recent publications[2, 14], the drain current calculation considering the complete distribution of DOS makes the drain current model complicated, which is the main obstacle in the drain current solution. Obtaining an explicit and accurate drain current expression is therefore the main target of this paper.

Following the charge-sheet approximation, the drain current including both drift and diffusion components from subthreshold to strong inversion regions can be rewritten as

$$I_{\rm ds} = -\frac{W}{L}\mu_{\rm eff}\left\{\int_{\psi_{\rm s0}}^{\psi_{\rm sL}} Q_{\rm i}(\psi_{\rm s}){\rm d}\psi_{\rm s} - \phi_{\rm t}[Q_{\rm i}(\psi_{\rm sL}) - Q_{\rm i}(\psi_{\rm s0})]\right\}, \quad (5)$$

where $\psi_{\rm sL}$ and $\psi_{\rm s0}$ are the surface potential obtained by Eq. (4), but with the different $\phi_{\rm n}$ concerning the source voltage and drain voltage, respectively. W is the gate width, $Q_{\rm i}$ is the charge per unit area, and $\mu_{\rm eff}$ is the unified field effect mobility.

Using the charge-sheet model[15] and following the charge neutrality condition, $Q_{\rm i}$ can be expressed as

$$Q_{\rm i}(\psi_{\rm s}) = -C_{\rm ox}(V_{\rm g}-V_{\rm fb}-\psi_{\rm s}) + qN_{\rm DS}t_{\rm film} + qN_{\rm TA}t_{\rm film}, \quad (6)$$

where $N_{\rm TA}$ and $N_{\rm DS}$ are the density of the trap states for exponential and monoenergetic traps, respectively, and $t_{\rm film}$ is the depleted thickness of the poly-Si thin film. Herein, since the polysilicon film is thin, the bulk charge density can be considered to be constant in the whole operation region. Although this assumption is less physical, it makes the integral in Eq. (5) simple and the explicit solution of drain current workable, the validity of which is also shown by Ref. [5].

The density of the accept-like exponential band-tail states at the surface can be expressed as[15]

$$N_{\rm TA} = g_{\rm c1}\frac{\pi kT}{\sin(\pi kT/E_1)}\exp\frac{q\psi_{\rm s}-q\phi_{\rm n}+E_{\rm f}-E_{\rm c}}{E_1}. \quad (7)$$

Besides, the density of the monoenergetic deep states at the surface, is expressed as[5]

$$N_{\rm DS} = \frac{N_{\rm T}}{1+K_{\rm m}\exp(-q\psi_{\rm s}/kT)}. \quad (8)$$

Substituting Eq. (6) into Eq. (5) and integrating, the analytical expression of drain current can be obtained as

$$I_{\rm ds} = -\frac{W}{L}\mu_{\rm eff}\{[g(\psi_{\rm sL}) - g(\psi_{\rm s0})] - \phi_{\rm t}[Q_{\rm i}(\psi_{\rm sL}) - Q_{\rm i}(\psi_{\rm s0})]\}, \quad (9)$$

where

$$\begin{aligned} g(\psi_{\rm s}) &= \int Q_{\rm i}(\psi_{\rm s}){\rm d}\psi_{\rm s} \\ &= -C_{\rm ox}[(V_{\rm g}-V_{\rm fb})\psi_{\rm s} - 0.5\psi_{\rm s}^2] \\ &\quad - qt_{\rm film}\left[N_{\rm T}\phi_{\rm t}\ln\left(1+K_{\rm m}\exp\frac{-\psi_{\rm s}}{\varphi_{\rm t}}\right) + N_{\rm T}\psi_{\rm s}\right] \\ &\quad - qt_{\rm film}N_{\rm TA0}\frac{E_1}{q}\exp\frac{\psi_{\rm s}}{E_1/q}. \end{aligned}$$

When the proposed model is applied to the short channel devices, short channel effects such as the DIBL effect, the kink effect and mobility must have been taken into account. The precise modeling of the above effects is beyond the scope of this paper, and the reader can be referred to Refs. [10, 15] for an extensive treatment of this subject. Nevertheless, for the sake of completeness, the influence of the above-mentioned effects on drain current will be briefly discussed as follows.

The effective mobility affected by gate voltage is given by[15]

$$\mu_{\rm eff} = \mu_{\rm s} + \frac{\mu_{\rm h}\exp\dfrac{-V_{\rm b}}{\phi_{\rm t}}}{1+\theta_1(V_{\rm g})^{1/3}+\theta_2(V_{\rm g})^2} \quad (10)$$

with

$$V_{\rm b} = \left[\left(V_{\rm gb}-V_{\rm i}\right)^2 + (V_{\rm Q}-\kappa V_{\rm ds})^2\right]^{1/2} - \left(V_{\rm gb}-V_{\rm i}\right), \quad (11)$$

where $\mu_{\rm s}$ and $\mu_{\rm h}$ are the channel mobility in the subthreshold and inversion regions, θ_1 and θ_2 are the mobility degradation parameters, $V_{\rm Q}$ and $V_{\rm i}$ are the fitting potential barrier height parameters, while $V_{\rm gb} = V_{\rm g} - V_{\rm fb}$, κ is a parameter concerning the channel length L when the drain-induced grain barrier lowering (DIGBL) effect is taken into account[15].

For considering the DIBL effect, the gate voltage V_g must be replaced by $V_g + \sigma V_{ds}$ in the calculation of the surface potential and mobility in Eqs. (9) and (10).

In addition, for taking the kink effect into account, the multiplication factor M is needed for the expression of the drain current model. Therefore, it yields[15]

$$M = A[V_{ds} - (\psi_{sL} - \psi_{s0})] \exp \frac{-B}{V_{ds} - (\psi_{sL} - \psi_{s0})}, \quad (12)$$

where A and B are the process-dependent fitting parameters. In short, when taking the short channel effects into consideration, the drain current model can be regarded as

$$I_{ds} = -\frac{W}{L}\mu_{eff}(1+M) \times \{[g(\psi_{sL}) - g(\psi_{s0})] - \varphi_t[Q_i(\psi_{sL}) - Q_i(\psi_{s0})]\}. \quad (13)$$

It is clear that the drain current model of Eq. (13), based on surface potential, is inherently single-piece without smoothing function, and gives an accurate and continuous description of current in all operation regions above flat-band voltage. Furthermore, due to the use of the explicit formulation of surface potential, the analytical expression of Eq. (13) without numerical calculations improves the simulation time, which is important for circuit simulators.

4. Trap state distribution

As shown in Section 3, drain current characteristics are particularly dependent on the distribution of the trap states. Therefore, a new parameter extraction of trap state distribution obtained by the OEMS response current is developed. Under the conditions of the OEMS measurement, the first-order solution of electronic density in trap states n_t is achieved by[16]

$$n_t = -N_T f(hv) \frac{\Phi \Delta\beta \tau_{on}}{1 + j\omega_m \tau_{on}}, \quad (14)$$

where $f(hv)$ is the average trap occupation probability, τ_{on} is the light response time which describes a time delay between the response and the changing of the channel current, ω_m is the angle frequency of incident light, Φ is the photon flux density and $\Delta\beta$ characterizes the optical emission rate variation with energy. Similarly, the response for band-tail states is expressed as[16]

$$\Delta n(W_m) = -N_{TA} f(W_m) \Delta W_m \frac{\Phi \Delta\beta \tau_{on}}{1 + j\omega_m \tau_{on}}, \quad (15)$$

where ΔW_m is the optical measurement range.

The OEMS current response spectrum of the poly-Si TFTs can be seen in Ref. [4]. The transistor is a weak n-type. In the OEMS measurement, the devices not only work in depletion mode but also in the subthreshold region in order to obtain the information of the trap states. Thus, to the monoenergetic deep-level states, following the Gaussian law $\frac{d^2\psi}{dx^2} = -\frac{q}{\varepsilon_{si}} \frac{N_T}{1+K_m \exp(-q\psi/kT)}$, using Ohm's law and gradual channel approximation, the response current of the monoenergetic deep-level states, can be expressed as

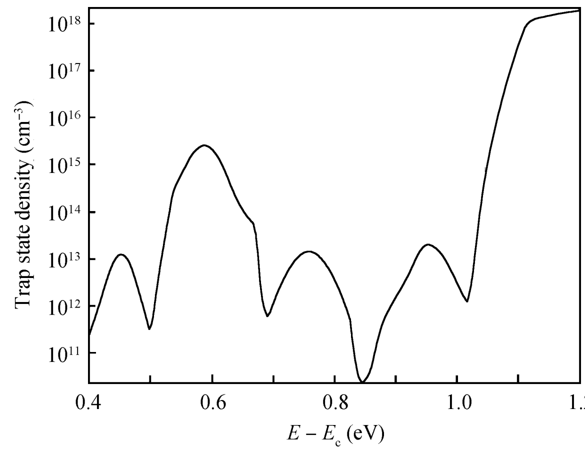

Fig. 1. Distribution of the trap states.

$$I_m = \frac{\mu W B(\psi)}{L} V_{ds} N_T f(hv) \frac{\Delta\beta \Phi \tau_{on}}{1 + j\omega_m \tau_{on}}, \quad (16)$$

where $B(\psi) = \{2q\varepsilon_{si}[\psi + \phi_t \ln(1+K_m) - \phi_t \ln(1+K_m)]/N_T\}^{1/2}$, and the surface potential ψ is more approximate to the subthreshold one calculated by Eq. (2), V_{ds} is the drain–source bias, which is assumed to be sufficiently small for the channel to be regarded as parallel. To the band-tail states, following the similar law as the deep-level states, using the Poisson equation $\frac{d^2\psi}{dx^2} = -\frac{q}{\varepsilon_{si}} N_{TD}$, the response current for is derived as

$$I_m = \frac{\mu W[C(\psi_{sL}) - C(\psi_{s0})]}{L} \frac{q N_{TD} f(W_m) \Delta W_m}{\sqrt{\frac{2q}{\varepsilon_{si}} N_{TD0} \frac{E_1}{q}}} \frac{\Phi \Delta\beta \tau_{on}}{1 + j\omega_m \tau_{on}}, \quad (17)$$

where $N_{TD} = g_{v1} \frac{\pi kT}{\sin(\pi kT/E_1)} \exp \frac{E_v + q\psi - q\varphi_n - E_f}{E_1} = N_{TD0} \exp \frac{q\psi}{E_1}$ and g_{v1} is the p-type exponential trap state density, $C(\psi) = (\frac{2E_1}{q})^2(1 + \frac{2E_1}{q}) \exp \frac{-\psi}{2E_1/q} + \frac{2E_1}{q}\psi - (\frac{2E_1}{q})^2 \ln(V_g - V_{fb} - \psi)$, as known by Eqs. (16) and (17), and the response current is proportional to the density of the trap distribution and the optical emission rate which characterize the relations between the OEMS measurement results and the distribution of the trap states. When $V_{ds} = 4$ V, the distribution of the trap states, which is derived by the comparison between Eqs. (16) and (17), can be seen in Fig. 1, and has a number of deep-level trap states and exponential band-tail trap states within the band gap. ψ can be calculated by Eq. (4), and other parameters can be seen in the first validation in Table 1. The distribution is applied to the drain current model to make comparisons with the experimental data in order to verify its practicality.

5. Results and discussion

From Section 2, the surface potential can be extracted accurately by Eq. (4). It should be emphasized that the trap state density affects the I–V characteristics significantly. In Fig. 2, it is clear that the threshold voltage becomes higher with increasing trap density because the TFTs require a higher gate voltage to induce more free charge to fill up the trap in order to

Table 1. Simulation parameters.

Symbol	TFTs in Fig. 3[4]	TFTs in Fig. 4[10]	TFTs in Fig. 5[10]
E_1 (eV)	0.06	0.06	0.06
$g_{c1}(g_{v1})$ (cm^{-3}·eV^{-1})	2×10^{18}	2×10^{18}	2×10^{18}
N_T (cm^{-3})	5×10^{15}	2×10^{16}	2×10^{16}
E_T (eV)	0.01	0	0
μ_s (cm^2/(V·s))	0.15	10	10
μ_0 (cm^2/(V·s))	8	90	100
θ_1 (V$^{-1/3}$)	12×10^{-3}	4×10^{-3}	1×10^{-2}
θ_2 (V^{-2})	7.5×10^{-3}	2×10^{-4}	3×10^{-3}
κ	0	0.035	0.035
σ	0.01	0.01	0.06
A (V^{-1})	0.75	0.022	0.1
B (V)	9	4	6
V_{fb} (V)	0	0	0
V_Q (V)	0.95	0.4	0.4
V_i (V)	1	0.5	0.5
t_{film} (μm)	0.1	0.1	0.1

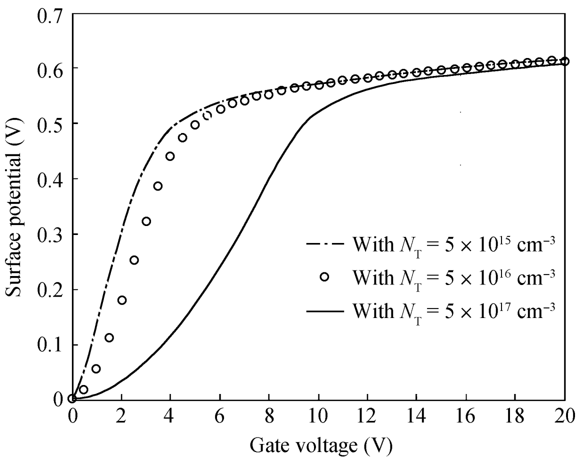

Fig. 2. Surface potential as a function of gate voltage.

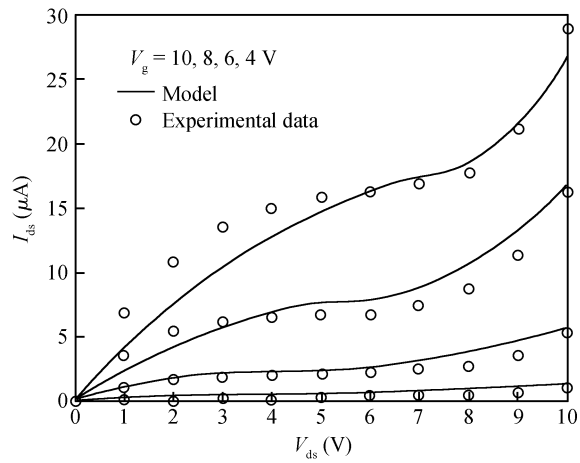

Fig. 3. Comparison of output characteristics between the model and experimental data (W/L is 150 μm/6 μm).

reach the inversion region, which is consistent with the drain current observations.

The drain current model, Eq. (13), which is based on the surface potential, can describe the I–V characteristics when the gate voltage is larger than the flat band voltage. In order to support the effectiveness of the drain current model, we compare our model with the available experimental data on different TFTs. The parameters of these TFTs used in the simulation are given in Table 1.

The first validation is achieved by comparing our model with experimental data from the Philips company, and using the trap states density obtained by the comparison between Eqs. (16) and (17). The structure and fabrication process are shown in Ref. [4]. In Fig. 3, it is clear that the comparisons of the output characteristics have a good fit to the experimental data. Furthermore, the model can also describe the characteristics accurately, including the kink effect under the large V_{ds}.

The second validation of the proposed model is investigated by comparisons with the experimental data from Ref. [10]. The density of trap states is different from the first validation because of the different fabrications. From the comparisons we can see that for the TFTs with different channel lengths, the behaviors of the devices are still well predicted by our model, including the DIBL and kink effects for the short channel devices. Specifically, the DIBL effect is often significant in the subthreshold region in the transfer characteristics. As a result, it is evident that due to the DIBL effect being significant to short channel devices, the increasing drain current with V_{ds} in Fig. 5(a) is more obvious than that in Fig. 4(a). Similarly, the increasing drain current of Fig. 5(b) with V_{ds} is more evident than that in Fig. 4(b) because the impact ionization in high electric fields impacts strongly in short channel devices.

6. Conclusions

In this work, a physical-based drain model drain current for poly-Si TFTs, valid in a wide range of channel length and operational regions, is proposed. First, the proposed model accounts for monoenergetic deep-level states around the midgap and an exponential distribution of DOS near the conduction or valence band edge. Second, the drain current model is analytical and single-piece, and valid in all operation regions above flat-

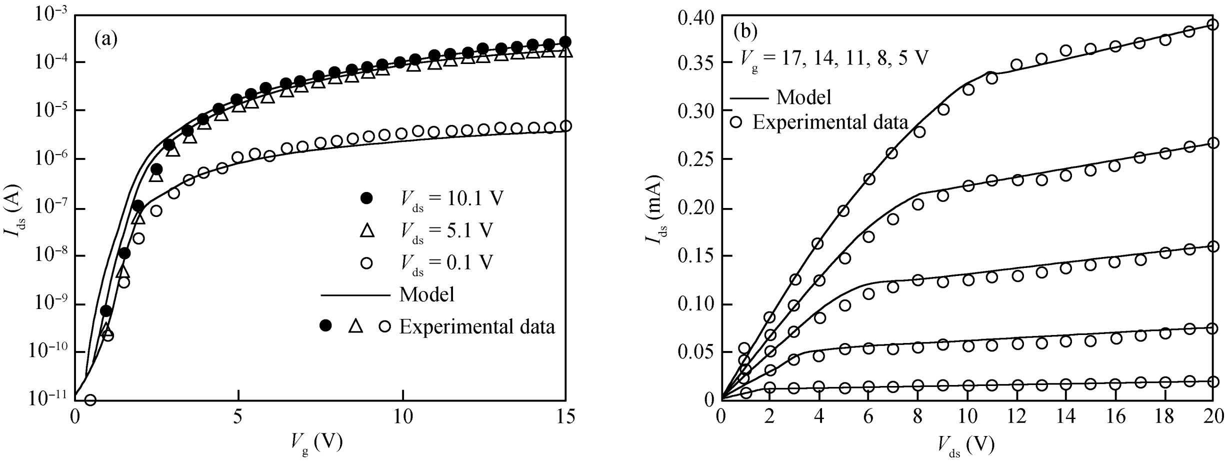

Fig. 4. Comparison of the drain current model and the experimental data with 50 μm/50 μm devices. (a) Transfer characteristics. (b) Output characteristics.

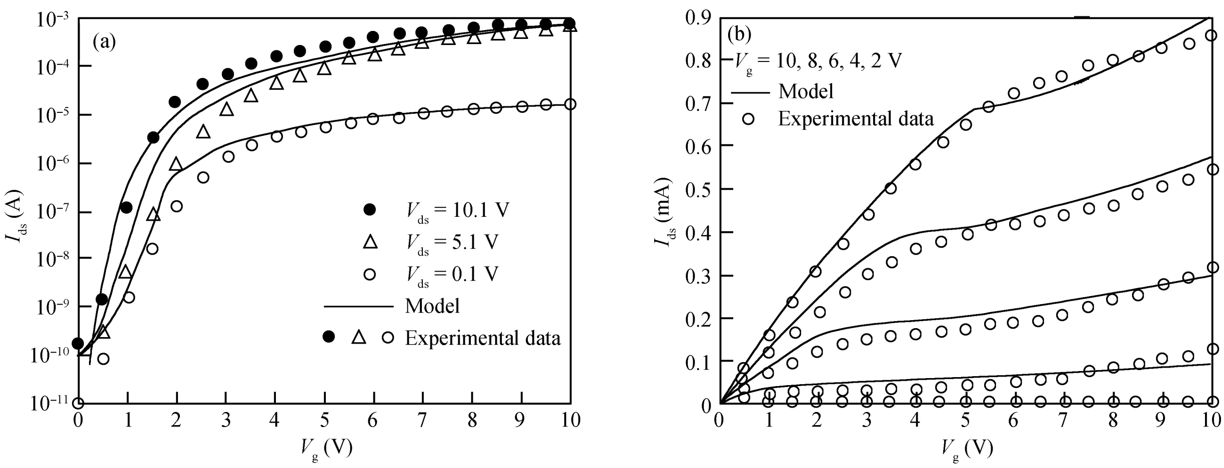

Fig. 5. Comparison of the drain current model and the experimental data with 50 μm/6 μm devices. (a) Transfer characteristics. (b) Output characteristics.

band voltage. Third, the calculations of the proposed model use non-iterative methods, which are suitable for circuit simulators. Fourth, the distribution of the trap states within the band gap is derived, and finally, such distribution is applied to the model and comparisons with the available experimental data are made. The results show that the drain current model of poly-Si TFTs is satisfactory for the various kinds of devices.

References

[1] Werner J, Persl M. Exponential band tails in polycrystalline semiconductor films. Phys Rev B, 1985, 31(10): 6881

[2] Dimitriadis C A, Tassis D H, Economou N A, et al. Determination of bulk states and interface states distribution in polycrystalline silicon thin film transistors. J Appl Phys, 1993, 74(4): 2919

[3] Jackson W B, Johnson N M, Biegelsen D K. Density of gap states of silicon grain boundaries determined by optical absorption. Appl Phys Lett, 1983, 43(2): 195

[4] Huang Junkai, Jiang Xiaozhou, Deng Wanling. Characterization of trap states distribution in poly-Si TFTs using OEMS. Symposium on Photonics and Optoelectronic, 2010: 5504394

[5] Chen Rongshen, Zheng Xuren, Deng Wanling, et al. A physics-based analytical solution to the surface potential of polysilicon thin film transistors using the Lambert W function. Solid-State Electron, 2007, 51(6): 975

[6] Qureshi S, Siddiqui M J. A DC charge sheet turn-on model for the I–V characteristics of doped polysilicon thin film transistors. Semicond Sci Technol, 2002, 17(6): 526

[7] Tsuji H, Kamakura Y, Taniguchi K. Drain current model for thin-film transistors with interface trap states. J Appl Phys, 2010, 107(3): 034502

[8] Ikeda H. Surface potential-based polycrystalline silicon thin-film transistor model. Jpn J Appl Phys, 2007, 46(6A): 3337

[9] Baccarani G, Ricco B, Spadini G. Transport properties of polycrystalline silicon film. J Appl Phys, 1978, 49(11): 5565

[10] Jacunski M D, Shur M S, Owusu A A, et al. A short channel DC SPICE model for polysilicon thin-film transistors including temperature effects. IEEE Trans Electron Devices, 1999, 46(6): 1146

[11] Iñiguez B, Zheng X, Tor A F, et al. Unified model for short-channel poly-Si TFTs. Solid-State Electron, 1999, 43(10): 1821

[12] Chen S S, Shone F C, Kuo J B. A closed-form inversion-type polycrystalline thin-film transistor DC/AC model considering the kink effect. J Appl Phys, 1995, 77(4): 1776

[13] Deng Wanling, Huang Junkai. A physics-based approximation

for the polysilicon thin-film transistor surface potential. IEEE Electron Device Lett, 2011, 32(5): 647
[14] Tsuji H, Kuzuoka H, Kishida Y, et al. Surface-potential-based drain current model for polycrystalline silicon thin-film transistors. Jpn J Appl Phys, 2008, 47(10): 7798
[15] Deng Wanling, Zheng Xueren, Chen Rongshen. A new poly-Si TFTs DC model for device characterization and circuit simulation. Chinese Journal of Semiconductors, 2007, 28(12): 1916
[16] Wang Q H, Swanson J H. Depletion mode optoelectronic modulation spectroscopy. J Appl Phys, 1996, 80(12): 6943